Kinetics and Mechanisms of Monolayer Interactions V: Surface Activities of Alkylamides, Alkylmonocarboxylic Acids, and Alkylketones and Their Interaction Energies with Phospholipid Monolayers

FEDERICO A. VILALLONGA ˣ **and EDWARD W. PHILLIPS**

Received May 2, 1979, from the *College of Pharmacy, University of Florida, Gainesville, FL 32610.* Accepted for publication July 24, 1979.

Abstract □ The adsorption free energies of the C_1–C_6 alkylamides, C_3–C_8 alkylketones, and C_1–C_{10} alkylmonocarboxylic acids at the air–water interface, estimated from plots of the surface pressure (≤5 dynes/cm) *versus* the bulk concentration, were linear functions of the total surface area per molecule (square angstroms per molecule), with a slope 46% higher for the alkylamides and 25% lower for the alkylketones than that for the monocarboxylic acids. The interaction energies of alkylamides with dipalmitoyl lecithin and dipalmitoyl phosphatidylethanolamine spread at the air–water interface, estimated from the surface pressure increase with increasing concentrations of the injected C_1–C_5 compounds, were linear functions of the total surface area per molecule. The diffusion free energies, ΔG_{dif}, of the alkylamides within a phospholipid bilayer, predicted from the permeability equation and their interaction energies with dipalmitoyl lecithin monolayers by assuming the additivity of their free energies of adsorption and dehydration at the solution–bilayer interface, agreed with the literature data.

Keyphrases □ Surface activity—alkylamides, alkylmonocarboxylic acids, and alkylketones, interaction energies with phospholipid monolayers □ Phospholipid monolayers—interaction energies with alkylamides, alkylmonocarboxylic acids, and alkylketones □ Interaction energies—alkylamides, alkylmonocarboxylic acids, and alkylketones with phopholipid monolayers

The adsorption free energies of alkanols at the air–aqueous interface estimated from plots of the surface pressure *versus* the bulk concentration were compared (1) with their interaction energies with dipalmitoyl lecithin (I) and dipalmitoyl phosphatidylethanolamine (II) monolayers, estimated from the variation of the equilibrium surface pressure with varying concentrations of subphase-injected alkanols based on a collision model and a constant entropy factor (2, 3).

The present work compares the adsorption free energies at the air–aqueous interface of alkylamides, their *N*-methyl derivatives, alkylmonocarboxylic acids, and alkylketones with those of the alkanols and with their interaction energies with I and II monolayers. Correlations between the surface activities and the molecular surface areas of the compounds are considered, and the implications with partition coefficients and permeabilities of these substances through biomembranes and liposomes are discussed.

EXPERIMENTAL

Reagents—Dipalmitoyl lecithin[1] and dipalmitoyl phosphatidylethanolamine[1] were homogeneous by TLC (4). Reagent grade formamide[2], acetamide[3], propionamide[4], butyramide[5], valeramide[2], hexanamide[2], *N*-methyl-[2] and *N,N*-dimethylformamide[2], *N*-methyl-[2] and *N,N*-dimethylacetamide[5], *N*-methyl-[2] and *N,N*-dimethylpropionamide[2], *N*-methyl-[6] and *N,N*-dimethylbutyramide[6], *N,N*-dimethylvaleramide[2], *N,N*-dimethylhexanamide[2], formic acid[4], propionic acid[3], butyric acid[5], valeric acid[5], hexanoic acid[5], octanoic acid[5], decanoic acid[5], propanone[5], 2-butanone[5], 2-pentanone[5], 2-hexanone[5], and 2-octanone[5] were used without further purification. The hexane[7] used to prepare the spreading solution and the distilled water used to prepare the aqueous solution and as a subphase for the phospholipid monolayers fulfilled the requirements described previously (2, 3).

Instruments—A 9-cm diameter polytef dish with two identical microburets[8] and a polytef-coated stirring bar (1.25 × 0.8 cm) was used as a trough in the closed system described previously (2, 3). Surface tension was measured with a Wilhelmy platinum plate (2.5 × 1.25 × 0.01 cm) attached to an electrobalance[9] whose output was fed into a recorder[10].

Surface Tensions of Aqueous Solutions—The surface tension of the aqueous solutions was measured as described previously (1). The reproducibility was within ±0.2 dyne/cm. All experiments were performed at 21 ± 1°. The surface pressure, π, obtained by the difference between the previously determined surface tension of the pure water and the surface tension of the aqueous solution, was fitted to an exponential function of the concentration, C (moles per liter), by digital computerized nonlinear regression (1). The Gibbs adsorption equation was used in the form described previously (1):

$$\Gamma_2 = \frac{d\pi}{d \ln C_2}\left(\frac{1}{kT}\right) \qquad \text{(Eq. 1)}$$

where Γ_2 is the solute surface concentration (molecules per square centimeter), π is the surface pressure (dynes per centimeter), C_2 is the solute concentration in the bulk solution (moles per liter), k is the Boltzmann constant (ergs per molecule per degree), and T is the absolute temperature (°K). The derivative ($d\pi/d \ln C_2$) of the exponential function that approximates the surface pressure dependence on concentration was computed with respect to the logarithm of the concentration. Substitution of these values into Eq. 1 permitted calculation of Γ_2 at any C_2.

Injection under Phospholipid Monolayers—Spreading of the phospholipid monolayers and injection of the test substance were performed as described previously (1–3). The initial phospholipid monolayer surface pressure was 5 ± 0.1 dynes/cm in all experiments. The criterion of equilibrium after the injection of the studied substance was the constancy (±0.1 dyne/cm) of the surface pressure increment, $\Delta\pi$, during 30 min.

RESULTS

Adsorption at Clean Air–Aqueous Interface—Typical plots of the surface pressure *versus* the logarithm of the concentration for some compounds are given in Figs. 1–4. Plots of surface pressure *versus* log concentration obtained with 0.1 *M* HCl solutions of the alkylmonocarboxylic acids coincided with those of their pure water solutions within reproducibility limits.

The standard free energy change, ΔG°_{ad} (ergs per molecule), associated with solute adsorption at the clean air–aqueous interface was estimated from (1, 5):

$$\Delta G^\circ_{ad} = -kT \ln \frac{\pi}{x_2^*} \qquad \text{(Eq. 2)}$$

where x_2^* is the solute activity. The ΔG°_{ad} values were calculated from the slope (π/x_2^*) of the plot of π (≤5 dynes/cm) *versus* the solute mole fraction

[1] Mann Research Laboratories, Orangeburg, N.Y.
[2] Pfalz and Bauer, Stanford, Conn.
[3] J. T. Baker Chemical Co., Rochester, N.Y.
[4] Eastman Kodak Co., Rochester, N.Y.
[5] Aldrich Chemical Co., Milwaukee, Wis.
[6] Prepared by K. V. Rao.
[7] Matheson, Coleman and Bell, East Rutherford, N.J.
[8] Manostat, New York, N.Y.
[9] Cahn Division, Ventron Instruments Corp., Paramount, Calif.
[10] Leeds and Northrup, North Wales, Pa.

0022-3549/80/0100-0065$01.00/0

Table I—Total Molecular Surface Area, Adsorption Free Energies at the Air–Water Interface, ΔG°_{ad}, and Interaction Energies, ψ, with I and II Monolayers

Compound	TSA, Å²/molecule	Air–Water			I-Water,	II-Water,
		r	$\frac{\pi}{X_2}$	$-\Delta G^{\circ}_{ad} \times 10^{13}$, ergs/molecule	$\psi_I \times 10^{13}$, ergs/molecule	$\psi_{II} \times 10^{13}$, ergs/molecule
Formamide	64.2	0.9945	39.0	1.5	0.3	0.7
Acetamide	84.6	0.9916	1.8×10^2	2.1	0.6	1.3
Propionamide	103.1	0.9889	1.7×10^3	3.0	1.3	2.3
Butyramide	121.3	0.9833	7.7×10^3	3.6	2.2	2.9
Valeramide	139.4	0.9967	2.0×10^4	4.0	2.5	3.5
Hexanamide	157.5	0.9999	3.1×10^4	4.4	3.2	3.5
N,N-Dimethylformamide	105.9	0.9923	8.9×10^2	2.8	0.7	1.1
N,N-Dimethylacetamide	121.7	0.9892	1.4×10^3	2.9	1.0	1.3
N,N-Dimethylpropionamide	140.3	0.9875	3.3×10^3	3.3	—	—
N,N-Dimethylbutyramide	158.4	0.9797	1.0×10^4	3.8	1.8	1.8
N,N-Dimethylvaleramide	176.5	0.9952	3.4×10^4	4.3	2.0	2.1
N,N-Dimethylhexanamide	194.7	0.9975	1.2×10^5	4.7	2.3	3.2
Formic acid	59.1	0.9977	2.7×10^2	2.3	0.6	1.0
Acetic acid	73.7	0.9979	1.2×10^3	3.1	0.9	1.0
Propionic acid	98.1	0.9969	3.2×10^3	3.3	1.6	1.5
Butyric acid	116.2	0.9974	2.0×10^4	4.0	2.2	2.5
Valeric acid	134.3	0.9998	7.0×10^4	4.5	3.0	3.2
Hexanoic acid	152.5	0.9967	1.2×10^5	4.8	3.5	3.4
Octanoic acid	188.7	0.9983	1.2×10^6	5.7	4.4	4.8
Decanoic acid	261.3	0.9368	1.9×10^7	6.8	—	—
Propanone	82.0	0.9967	1.3×10^3	2.9	0.8	1.2
2-Butanone	109.2	0.9966	3.4×10^3	3.3	0.7	1.4
2-Pentanone	127.2	0.9961	5.2×10^3	3.5	0.9	1.6
2-Hexanone	145.4	0.9838	8.8×10^3	3.7	2.2	2.1
2-Octanone	181.6	0.9968	9.0×10^4	4.6	—	3.0
Methanol	61.9	0.9972	4.7×10^2	2.5	0.0	0.2
Ethanol	79.6	0.9983	1.3×10^3	2.9	0.7	0.9
Propanol	99.7	0.9983	4.0×10^3	3.4	1.2	1.5
Butanol	115.8	0.9994	1.1×10^4	3.8	1.7	1.9
Pentanol	134.0	0.9998	4.0×10^4	4.3	2.4	2.3
Hexanol	152.1	0.9922	1.1×10^5	4.7	3.6	4.2
Heptanol	170.3	0.9999	3.3×10^5	5.2	3.8	4.6
Octanol	188.4	0.9917	1.2×10^6	5.7	4.3	4.7

in the bulk solution, x_2, when $x_2 \rightarrow 0$ and $x_2^* \rightarrow x_2$ at low mole fractions. For all compounds, plots of the surface pressure ($\pi \leq 5$ dynes/cm) *versus* the solute mole fraction in the bulk solution were reasonably linear. The correlation coefficients (r), the slopes, and the estimated ΔG°_{ad} values obtained from such plots are given in Table I.

It was shown previously (1) that the simultaneous effect of the chain length and the position of the hydroxyl group on the alkanol surface activity is described best by the total molecular surface area, TSA (square angstroms per molecule), of the alkanol molecule. Molecular surface areas of the compounds were calculated by a modified version (6) of the original computer program MOLAREA (7). The molecule was considered as a collection of spherical groups and individual atoms. The methyl, methylene, and hydroxyl groups were approximated as single spheres, and standard geometry and interatomic bond lengths and angles (8, 9) were used in the construction of the molecules. These molecular surface areas are listed in Table I.

Plots of ΔG°_{ad} *versus* the total molecular surface area of alkylamides, their *N*-methyl derivatives, alkylmonocarboxylic acids, and alkylketones are compared in Fig. 5 with those for the alkanols. The experimental points yielded reasonably straight lines within the estimated experimental error (0.14 erg/molecule or 0.2 kcal/mole). The correlation coefficients and the slopes are listed in Table II.

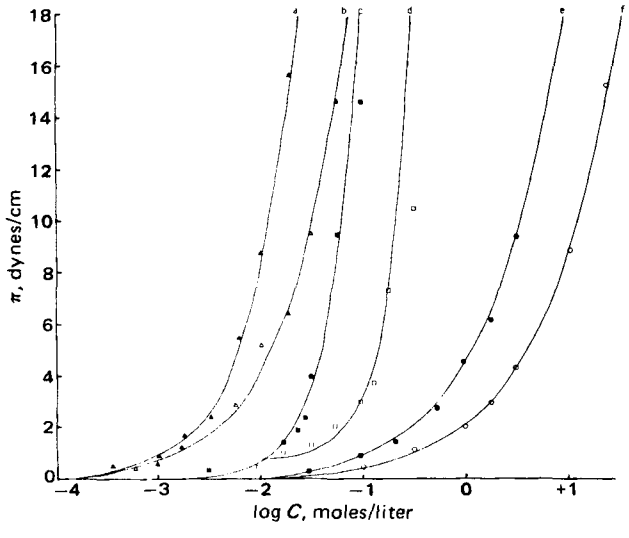

Figure 1—*Plots of the surface pressure, π, against the logarithm of the bulk concentration, C, for alkylamides from C_1 to C_6. Key: a, hexamide; b, valeramide; c, butyramide; d, propionamide; e, acetamide; and f, formamide. The lines through the experimental points were the best fit obtained with the computer (1).*

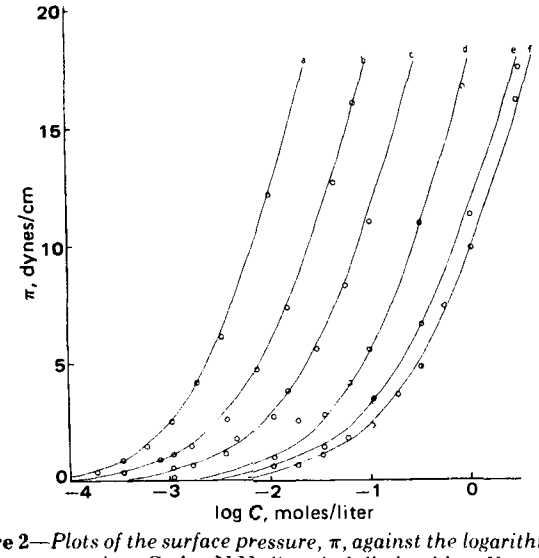

Figure 2—*Plots of the surface pressure, π, against the logarithm of the bulk concentration, C, for N,N-dimethylalkylamides. Key: a, N,N-dimethylhexanamide; b, N,N-dimethylvaleramide; c, N,N-dimethylbutyramide; d, N,N-dimethylpropionamide; e, N,N-dimethylacetamide; and f, N,N-dimethylformamide. The lines through the experimental points were the best fit obtained with the computer (1).*

Table II—Adsorption Free Energies per Methylene Group, ΔG_{CH_2}, at the Air–Water and Hydrocarbon–Water Interfaces, Interaction Energies per Methylene Group, ψ_{CH_2}, with I and II Monolayers, and Transfer Free Energies per Methylene Group, $\Delta G_{tr_{CH_2}}$, from Water to Oil

	Air–Water			Decane–[a] or Petroleum Ether[b]–Water			I–Water			II–Water			Oil–Water[c]		
Series	r	$\frac{\Delta G^\circ}{TSA}$, ergs/Å^2 × 10^{15}	$\Delta G^\circ_{CH_2}$, kcal/mole	r	$\frac{\Delta G_{ad}}{TSA}$, ergs/Å^2, × 10^{15}	$\psi G^\circ_{CH_2}$, kcal/mole	r	$\frac{\psi}{TSA}$, ergs/Å^2 × 10^{15}	ψ_{CH_2}, kcal/mole	r	$\frac{\psi}{TSA}$, ergs/Å^2 × 10^{15}	ψ_{CH_2}, kcal/mole	r	ΔG°_{tr}, ergs/Å^2 × 10^{15}	$\Delta G^\circ_{tr_{CH_2}}$, kcal/mole
Alkanols (C_1–C_5)[d]	0.9993	2.53	0.66	0.9954	3.26	0.85[b]	0.9942	3.21	0.84	0.9863	2.89	0.75	0.9983	3.0	0.79
Alkylketones (C_3–C_8)[d]	0.9638	1.65	0.43	—	—	—	—	—	—	—	—	—	0.9995	3.1	0.81
Alkylmonocarboxylic acids (C_1–C_{10})[d]	0.9750	2.20	0.57	—	—	—	0.9930	3.07	0.80	0.9817	3.35	0.87	0.9874	2.7	0.71
Alkylamides (C_1–C_6)[d]	0.9811	3.21	0.84	0.9997	3.22	0.84[a]	0.9803	3.25	0.85	0.9909	3.85	1.00	0.9831	3.2	0.83
N-Methylalkylamides (C_1–C_6)[d]	0.9811	2.26	0.59	—	—	—	—	—	—	—	—	—			
N,*N*-Dimethyl alkylamides (C_1–C_6)[d]	0.9811	2.27	0.59	—	—	—	0.9910	1.83	0.48	0.9979	1.4	0.37			

[a] From Ref. 31. [b] From Ref. 12. [c] From Ref. 33. [d] Number of carbon atoms in the hydrocarbon chain.

The slopes of the plots of the alkylmonocarboxylic acids and the *N*-methyl- and *N*-dimethylalkylamides were 13 and 10% smaller than those of the alkanols, respectively. The slopes of the plots of the alkylamides and alkylketones were 27% greater and 35% smaller than those of the alkanols, respectively.

Interaction with Phospholipid Monolayers—The interaction energies, ψ, were estimated from the slopes of the plots of the reciprocals of the equilibrium surface pressure, $\Delta\pi_{eq}$, after injection *versus* the reciprocals of the final concentration, n (molecules per cubic centimeter), of the subphase-injected substance (1–3). They are listed in Table I and are plotted in Figs. 6 and 7 *versus* the total surface area per molecule.

The plots for I monolayers were reasonably linear for alkylmonocarboxylic acids (C_1–C_8) and alkylamides (C_1–C_6) and their *N*-dimethyl derivatives. The interaction energies per methylene group, ψ_{CH_2}, estimated from the slopes of the plots of alkylmonocarboxylic acids and alkylamides (Table II), were similar to those of the alkanols (7), but the interaction energy of the *N*-dimethylalkylamides was 50% smaller.

For II monolayers, the interaction energies of formic acid, hexanamide, and *N*,*N*-dimethylhexanamide presented gross departures from linearity. The interaction energies per methylene group were higher for alkylamides and alkylmonocarboxylic acids and smaller for *N*-dimethylalkylamides than those of the alkanols.

The interaction energies of the first three compounds of the alkylketone series with I monolayers showed the same value within the estimated experimental error. In the interaction with II monolayers, the correlation coefficient was 0.93.

DISCUSSION

Adsorption at Clean Air–Aqueous Interface—From one compound of each of the studied homologous series to the next compound, there was a constant surface area increase of the hydrophobic moiety that progressively changed the hydrophilic–hydrophobic balance of the molecules. The slopes of the linear plots of the adsorption free energy *versus* the total

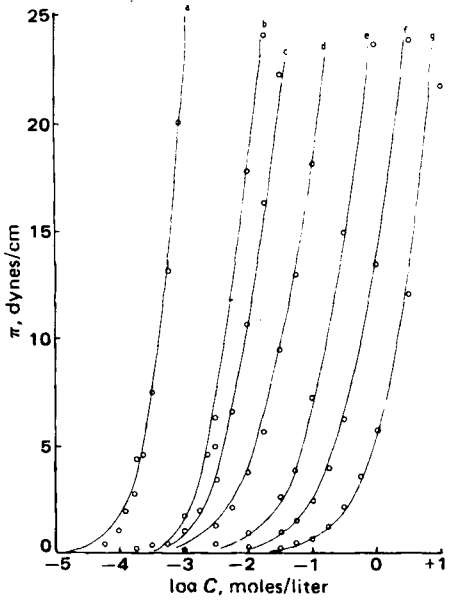

Figure 3—*Plots of the surface pressure, π, against the logarithm of the bulk concentrations, C, for alkylmonocarboxylic acids from C_1 to C_8. Key: a, octanoic; b, hexanoic; c, valeric; d, butyric; e, propanoic; f, acetic; and g, formic. The lines through the experimental points were the best fit obtained with the computer (1).*

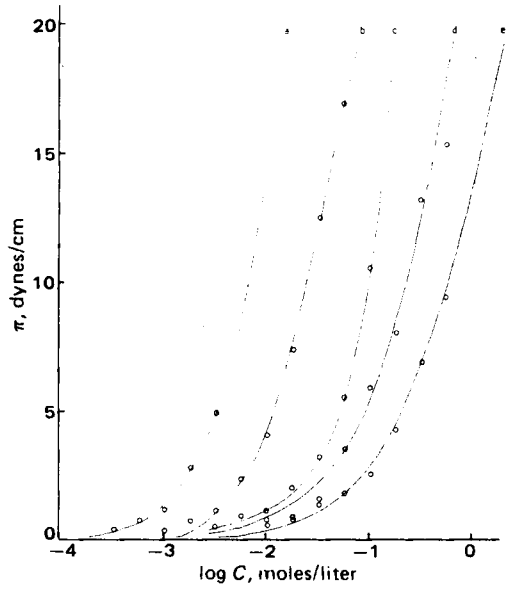

Figure 4—*Plots of the surface pressure, π, against the logarithm of the bulk concentration, C, for alkylketones from C_3 to C_8. Key: a, 2-octanone; b, 2-hexanone; c, 2-pentanone; d, 2-butanone, and e, propanone. The lines through the experimental points were the best fit obtained with the computer (1).*

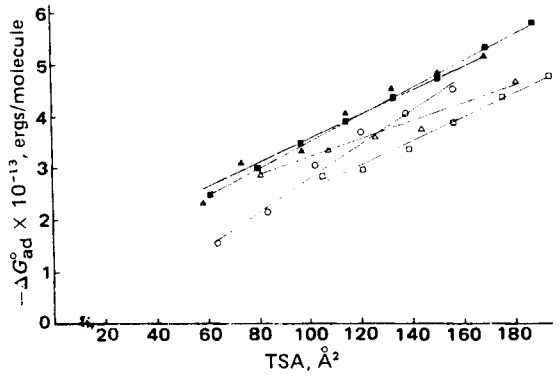

Figure 5—*Plots of the adsorption free energy of the air–aqueous solution interface, ΔG°_{ad} (ergs per molecule), against the total molecular surface area (square angstroms per molecule). Key: ▲, alkylmonocarboxylic acids; ■, alkanols; △, alkylketones; ○, alkylamides; and □, N,N-dimethylalkylamides.*

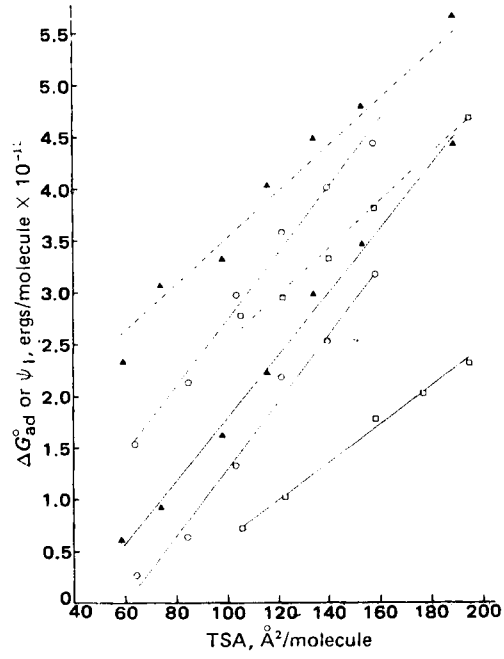

Figure 6—*Plots of the adsorption free energies at the air–aqueous solution interface (- - -) and of interaction energies with I monolayers (—) versus the total molecular surface area. Key: ▲, alkylmonocarboxylic acids; ○, alkylamides; and □, N,N-dimethylalkylamides.*

molecular surface area thus represent the contribution of each square angstrom increment of the hydrophobic surface area of the molecules to their total adsorption free energy.

The contribution to the molecular surface area due to an incremental methylene group in a straight chain extended conformation was estimated recently to be 18.1 Å² (6). The adsorption free energies per methylene group, ΔG_{CH_2}, of the studied homologous series calculated using this surface area contribution are listed in kilocalories per mole in Table II.

Since early findings obtained mainly with aliphatic alcohols, acids, and their esters (10, 11) were confirmed by several subsequent studies (1, 12–15), it generally has been accepted that the adsorption free energy increase produced by an incremental methylene group addition to a saturated straight hydrocarbon chain that adsorbs at the air–water interface is between 0.600 and 0.625 kcal/mole. The average value (0.603 ± 0.07 kcal/mole) obtained in the present study (Table II) for alkanols, alkylmonocarboxylic acids, and *N*-dimethylalkylamides reasonably agreed.

It is difficult to understand why the slope corresponding to the plot of the adsorption free energy *versus* the total molecular surface area for the alkylamides is 39% higher and that of the alkylketones is 29% lower than the average value (0.603 ± 0.07 kcal/mole) obtained for the rest of the homologous series.

The possibility existed that a different polar group attached to the same hydrocarbon chain might cause a different charge to be transferred along the methylene groups of the hydrocarbon chain, thus altering their interaction with the solvent molecules. Molecular orbital calculations performed on isolated molecules of 23 selected alkylamides, alkylmonocarboxylic acids, and alkanols failed to show evidence of a charge perturbation of the methylene groups beyond the first that could account for the observed effects of the amide group.

The fact that the adsorption free energy per methylene group of the *N*-methyl- and *N,N*-dimethylalkylamides is practically the same as that of the alkanols and alkylmonocarboxylic acids seems to indicate that the unsubstituted amino (NH_2) group is responsible for the higher adsorption free energy per methylene group in amides. Of the studied series, the amide group presents the higher hydrogen bonding capability. On the basis of *ab initio* self-consistent field method (SCF) computations of various polyhydrates, evidence was presented (16) for the structure of formamide in aqueous solutions consistent with a model of four water molecules in the primary hydration sphere, two of them hydrogen bonded to the amino group acting as a proton donor.

The standard adsorption free energy, ΔG°_{ad} (Eq. 2), is the free energy change associated with the transfer of one molecule from infinite dilution in bulk solution to infinite dilution at the interfacial region (5) and thus is a measure of the work of transfer. Kinetic data obtained for the time-dependent effect of cetrimonium ions injected beneath an air–aqueous interface on the water surface tension showed (17) excellent fit and consistency with a model that postulates an intermediate compartment (subinterface) between the plane of the interface and the bulk aqueous solution. This compartment is assumed to be a thin region with a thickness of 10–10^3 water molecule diameters (18) where the water molecules are oriented in a given array (19–21). Consequently, adsorption might be assumed to be energetically equivalent to the transfer of a solute molecule from a normal water environment in the bulk solution to the subinterface region where the water molecules are abnormally oriented.

Solute molecules such as those studied in the present work may interact with water molecules through hydrogen bonding of the polar hydrophilic group and through London dispersion forces generated mainly from its hydrophobic moiety. The negative standard adsorption free energies of formamide (−2.2 kcal/mole), formic acid (−3.3 kcal/mole), and methanol (−3.6 kcal/mole) indicate that the spontaneous tendency to perform the transfer from the bulk solution to the subinterface increases in the order: methanol > formic acid > formamide. Methanol and formamide present the minimum and maximum capabilities, respectively, to hydrogen bond with water; therefore, these results seem to indicate that, for these short-chain molecules, a correlation exists between their adsorption free energies at the air–aqueous interface and the hydrogen bonding capability of their hydrophilic moieties. The facts that aqueous urea solutions showed (22) a negative excess surface concentration (*i.e.*, $\Delta G^{\circ}_{ad} > 0$) and that thiourea in aqueous solution showed a negative adsorption free energy in preliminary experiments performed in this laboratory seem to corroborate this hypothesis.

The increase of the hydrocarbon chain length increases the surface area of the hydrophobic moiety only, enhancing its interaction through London dispersion forces with the water molecules. It seems reasonable that, at a given chain length, the adsorption free energy difference provoked by the different hydrophilic groups should be minimized due to the preponderant effect of the hydrophobic moiety. The adsorption free energies of hexanol, hexanoic acid, and hexamide are −6.8, −6.9, and −6.3 kcal/mole, respectively, in accord with this expectation; however, even for this chain length, hexanamide shows a significantly smaller value.

Experiments performed in this laboratory showed that, at constant temperature, the surface tension of heptanol–heptane mixtures adheres to the additivity rule represented by:

$$\gamma_{12} = \gamma_1 X_1 + \gamma_2 X_2 \qquad \text{(Eq. 3)}$$

where γ_{12} is the surface tension of the mixture and γ_1, γ_2, X_1, and X_2 are the surface tensions in the pure state (26.4 and 20.6 dynes/cm) and the mole fractions of heptanol and heptane in the mixture, respectively.

The surface tension of an aqueous solution containing 5.8×10^{-5} mole fraction of heptanol is 55 dynes/cm at 20°; *i.e.*, the surface tension of pure water (72.6 dynes/cm) is decreased 23% by the initial presence in the bulk solution of approximately six heptanol molecules/10^5 water molecules. A heptanol–heptane mixture containing this same heptanol mole fraction has the same surface tension as pure heptane within experimental error. In this last case, Eq. 1 predicts that the heptanol concentration at the interface is identical to that of the bulk solution. This fact suggests that

Table III—Diffusion Free Energies, ΔG_{dif}, of Alkylamides within a Phospholipid Bilayer

Compound	K, water–ether	$P^a \times 10^5$, cm/sec	$\Delta G_{dif}^{\ddagger a}$, kcal/mole	$\frac{\lambda^2}{l}\left(\frac{kT}{h}\right) \times 10^{-4}$, cm/sec	$-\psi_I$, kcal/mole	$\Delta G_{tr}^{\circ} - \Delta G_{ad}^{\circ}$ (o/w), kcal/mole	$\Delta G_{dif}^{calc\ b}$, kcal/mole
Formamide	0.0014	7.8 ± 0.5	6.15	1.61	0.43	5.61	6.10
Acetamide	0.0025	2.4 ± 0.4	7.55	2.11	0.86	5.61	7.46
Propionamide	0.013	6.1 ± 0.6	7.90	2.36	1.87	5.61	7.98
Valeramide	0.23	18.3 ± 1.1	8.00	2.98	3.60	5.61	9.18

[a] From Ref. 26. [b] Calculated from the equation: $\Delta G_{dif} = kT \ln [(\lambda^2/l)(kT/h)] + \psi_I - [\Delta G_{tr}^{\circ} - \Delta G_{ad}^{\circ}(o/w)] - kT \ln P$.

the different surface tension effects of the solvent produced by the presence of the same number of solute molecules in the two solutions may be related to some differential property between the water and heptane solvents.

The surface tension of a pure liquid is essentially a manifestation of the unbalanced molecular interactions on the surface molecules. The main intermolecular forces in liquid hydrocarbons are London dispersion forces. The hydrogen bond and London dispersion forces are the main intermolecular forces in water. The hydrogen bond component has been estimated to be responsible for two-thirds of the total surface energy of water (23).

The difference between the effect of heptanol on the surface tension of water and heptane could be related to the effect on the hydrogen bond component of the surface energy of water. The total molecular surface area of heptanol and the accepted water molecule radius (1.5 Å) lead to an estimated 25 water molecules packed closely around a heptanol molecule; *i.e.*, only 25 × 6 molecules out of 10^5 water molecules in this solution can be affected directly by the presence of heptanol molecules at that concentration.

If the assumption that the subinterface compartment with water molecules oriented in a given array (and, consequently, in a comparatively low entropic state) is valid, a plausible explanation of the magnitude of the observed effect on water could be that direct solute molecule interaction with a relatively small number of water molecules generates and propagates significant disruption of the water structure in the bulk solution. The entropic contribution thus created could be the driving force of the spontaneous heptanol molecule adsorption at the air–aqueous solution interface.

Interaction with Phospholipid Monolayers—Plots of the interaction energies, ψ, of alkylamides, *N*-dimethylalkylamides, and alkylmonocarboxylic acids with I monolayers *versus* the total molecular surface area are compared in Fig. 6 with those of their adsorption free energy at the clean air–water interface. The regression coefficients, the slopes, and the adsorption free energy per methylene group are listed in Table II.

The linearity of the plots of the compounds from C_1 to C_6 in the main hydrocarbon chain of the alkylamide and *N*-dimethylalkylamide series and from C_1 to C_8 in the alkylmonocarboxylic acids contrasts with the reported departure from linearity observed for the C_6 and C_8 compounds of the alkanol series in their interaction with I monolayers (1).

The interaction energies per methylene group of the alkylamides and alkylmonocarboxylic acids were practically identical to the adsorption free energies per methylene group at the hydrocarbon–water interface. This finding seems to indicate that I monolayers behave as ultrathin oil phases for these compounds, as was observed previously with alkanols (1). The observed 50% reduction of the interaction energy per methylene group of the hydrocarbon chain of the *N*-dimethylalkylamides compared with that of the adsorption free energies at the clean air–water interface. No literature data were found on the adsorption free energy of these compounds at the hydrocarbon–water interface.

The plots corresponding to II monolayers (Fig. 7) indicate a marked departure from linearity for hexanamide and *N*-dimethylhexamide and compare with that reported recently (7) for hexanol and octanol in their interaction with I and II monolayers. The interaction free energies per methylene group compare with those of the interaction with I monolayers. The small differences observed within the experimental error could be reasonably attributed to the different molecular surface density of I and II monolayers.

Correlations with Permeability—Three important variables govern nonelectrolyte permeation across biomembranes: (*a*) the partition coefficient of the membrane–bathing solution, (*b*) the rate constant for entrance into the membrane from the aqueous environment, and (*c*) the diffusion coefficient within the membrane (24). Solute permeation across the lipid regions of biomembranes can be separated into three successive events that contribute to the total permeation rate: (*a*) adsorption of the hydrated solute at the lipid–bathing solution interface, (*b*) dehydration, and (*c*) solute diffusion through the lipid region (25).

Kinetic analysis of membrane permeability (26, 27) based on the absolute rate theory treatment of diffusion (28) shows the permeation rate to be proportional to the product of the probability of occurrence of the three successive events (25):

$$P = \left(\frac{\lambda^2}{l}\right)\left(\frac{kT}{h}\right) \exp(-\Delta G_{ad}/RT) \exp(-\Delta G_{deh}/RT) \exp(-\Delta G_{dif}/RT) \quad \text{(Eq. 4)}$$

where P is the permeability (centimeters per second), λ is the average distance between equilibrium positions (angstroms), l is the membrane thickness (angstroms), h is the Planck constant (ergs × seconds), and ΔG_{ad}, ΔG_{deh}, and ΔG_{dif} are the contributions to the total activation energy of the adsorption, dehydration, and diffusion steps, respectively.

The ΔG_{ad} and ΔG_{deh} terms of Eq. 4 correspond to the first energetic barrier found by the solute molecule during its permeation, *i.e.*, the crossing of the bathing solution–lipid interface. Adsorption of the amides at the water–air or decane–water interface is spontaneous so that ΔG_{ad} is intrinsically negative. On the contrary, the nonspontaneity of dehydration indicates that ΔG_{deh} is intrinsically positive. Consequently, the total energetic cost of crossing the interfacial region is $-\Delta G_{ad} + \Delta G_{deh}$.

The free energy change, ΔG_{tr}, associated with the transfer of a solute from an aqueous solution to dimyristoyl lecithin liposomes was estimated by (29):

$$\Delta G_{tr}^{\circ} = -kT \ln P \quad \text{(Eq. 5)}$$

where P is the molal partition coefficient, which can be related to the thermodynamic partition coefficient through an expression containing

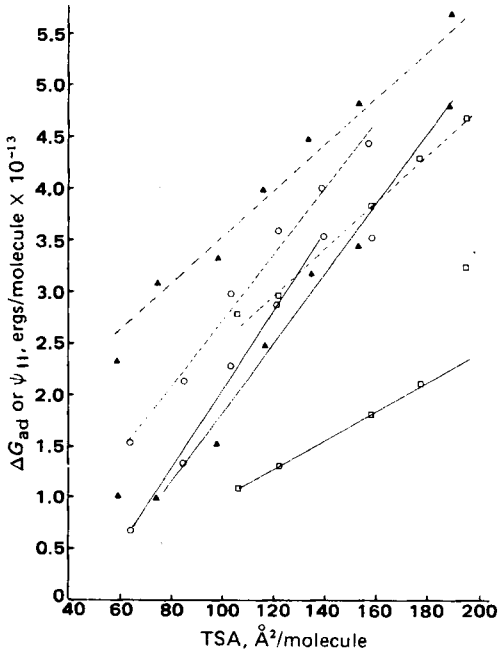

Figure 7—*Plots of the adsorption free energies at the air–aqueous solution interface (- - -) and the interaction energies with II monolayers (—)* versus *the total molecular surface area. Key:* ▲, *alkylmonocarboxylic acids;* ○, *alkylamides; and* □, N,N-*dimethylalkylamides.*

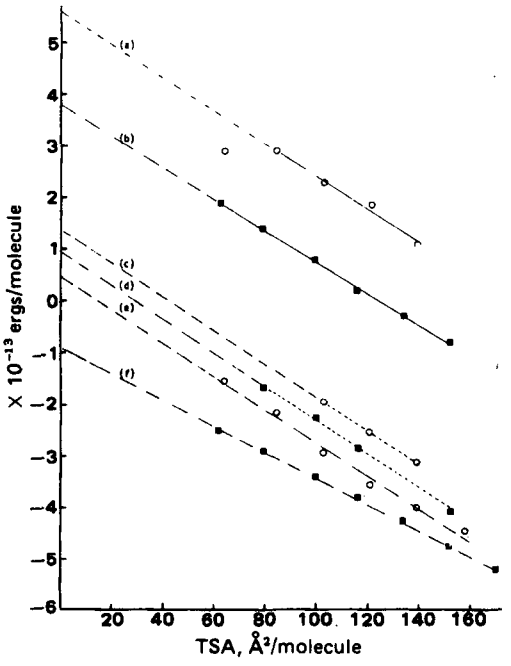

Figure 8—*Plots of the transfer free energies of the oil–water solution, ΔG°_{tr} (a, b); the adsorption free energies at the hydrocarbon–water interface, ΔG°_{ad} (o/w) (c, d); and the adsorption free energies at the air–water interface, ΔG°_{ad} (e, f), against the total molecular surface area. Key:* ○, *alkylamides; and* ■, *alkanols.*

the natural logarithm of the ratio of the molecular weights of the nonpolar and polar phases (29). However, for comparative purposes, the P values can be used to estimate a relative free energy change.

The plots of ΔG°_{tr} obtained from literature data (30) on partition coefficients of oil–aqueous solutions of alkylamides and alkanols *versus* the total surface area per molecule are compared in Fig. 8 with those of the adsorption free energy, $\Delta G^{o/w}_{ad}$, at the hydrocarbon–aqueous (obtained from Refs. 31 and 12, respectively) and at the air–aqueous interfaces. With the exception of formamide in the ΔG°_{tr} plot, the points determined reasonably straight lines. The slopes, intercepts, and correlation coefficient are given in Table II.

Parallelism of the plots of ΔG°_{tr} and ΔG°_{ad} at the hydrocarbon–water interface permitted estimation of the constant difference $(\Delta G^{\circ}_{tr} - \Delta G^{o/w}_{ad})_{TSA=0}$ for the alkylamides and the alkanols, 3.91×10^{-13} and 2.84×10^{-13} erg/molecule, respectively.

The partition of a surface-active solute between aqueous and nonaqueous phases can be separated into two successive events: the spontaneous adsorption of the hydrated solute at the interface ($\Delta G_{ad} < 0$) and its subsequent dehydration ($\Delta G_{deh} > 0$) that permits penetration into the nonaqueous phase (31). It can be reasonably assumed that the total free energy change of the partition, ΔG_{tr}, should reflect both events so that $\Delta G_{tr} = \Delta G^{o/w}_{ad} + \Delta G_{deh}$ and $\Delta G_{deh} = \Delta G_{tr} - \Delta G^{o/w}_{ad}$.

It is generally accepted (27, 32) that the amide group and the hydroxyl group form three and two hydrogen bonds with water, respectively. However, from *ab initio* SCF computations of various polyhydrates, evidence was presented recently (16) for the structure of formamide in aqueous solution consistent with a model of four water molecules in the primary hydration sphere, two of them hydrogen bonded to the amino group acting as a proton donor.

By assuming that the constant difference $(\Delta G^{\circ}_{tr} - \Delta G^{o/w}_{ad})_{TSA=0}$ is related to the free energy change that corresponds to dehydration, the contribution of each hydrogen bond to the total dehydration free energy can be estimated by dividing $(\Delta G_{tr} - \Delta G^{o/w}_{ad})_{TSA=0}$ by three for alkylamides and by two for alkanols. The values obtained, 1.31×10^{-13} and 1.42×10^{-13} erg/molecule, respectively, seem to indicate the validity of this assumption for the two series.

The equation used to estimate the interaction energies of subphase-injected solutes with phospholipid monolayers was derived originally (2) based on the statistical thermodynamic treatment of the Langmuir adsorption equation (33, 34). The Boltzmann–Maxwell exponential factor consequently contained an activation energy term about which, under the experimental conditions, no valid assumption could be made on the thermodynamic function (ΔE, ΔH, or ΔG) that it really represents. The ambiguous interaction energy term was coined, and the symbol ψ was used to represent it.

The order of magnitude of the experimentally measured interaction energies, ψ, of alkylamides and alkanols with phospholipid monolayers and their dependence on the total surface area per molecule strongly suggest that they could be related to the adsorption free energy of the solute at the phospholipid monolayer–aqueous solution interface. The validity of this suggested relationship and the former assumption of the dependence of ΔG_{deh} on $(\Delta G_{tr} - \Delta G^{o/w}_{ad})$ can be tested with Eq. 4.

The activation free energies for the diffusion, ΔG_{dif}, of formamide, acetamide, propionamide, and valeramide within egg lecithin bilayers estimated recently (26) from their measured permeability coefficients by assuming that the unknown bathing solution–lipid bilayer partition coefficients are proportional to the known water–ether partition coefficients are compared in Table III with those obtained by substituting ΔG_{ad} for the interaction energies with dipalmitoyl lecithin monolayers, ψ_I (Table I), and ΔG_{deh} for the corresponding values of $(\Delta G_{tr} - \Delta G^{o/w}_{ad})_{TSA=0}$ in Eq. 4. The coincidence of the calculated values of the activation free energy of the diffusion within the lipid bilayer for formamide, acetamide, and propionamide favors the validity of the former assumptions. The discrepancy between the calculated values of ΔG^{calc}_{dif} and $\Delta G^{\ddagger}_{dif}$ in the case of valeramide could be explained on the basis that as the solute size increases, the crossing of the interface becomes the rate-determining step; for valeramide, it constitutes 90% of the total resistance to permeation (24). The fact that in this case ΔG^{calc}_{dif} compares with ΔG°_{dif}, which contains the contribution corresponding to the partition coefficient $[\Delta G^{\circ}_{dif} = \Delta G^{\ddagger}_{dif} - \ln A/A'$ (24)], favors this explanation.

The results presented here seem to indicate that the interaction energy of alkylamides with dipalmitoyl lecithin monolayers spread at the air–water interface can be reasonably identified with the adsorption free energy at the aqueous solution–monolayer interface, which constitutes the first energetic step involved in alkylamide permeation across a phospholipid bilayer, and that the dehydration free energy constituting the second energetic step can be identified with the difference between the transfer free energy from an aqueous phase to an oil phase and the adsorption free energy at the water–hydrocarbon interface.

REFERENCES

(1) F. A. Vilallonga, E. R. Garrett, and J. S. Hunt, *J. Pharm. Sci.*, **66**, 1229 (1977).

(2) F. A. Vilallonga, E. R. Garrett, and M. Cereijido, *ibid.*, **61**, 1720 (1972).

(3) F. A. Vilallonga and E. R. Garrett, *ibid.*, **62**, 1605 (1973).

(4) G. M. Adams and T. L. Sallee, *J. Chromatogr.*, **49**, 552 (1970).

(5) J. H. Clint, J. M. Corkill, J. F. Goodman, and J. A. Tate, *J. Colloid Interface Sci.*, **28**, 522 (1968).

(6) S. C. Valvani, S. H. Yalkowsky, and G. L. Amidon, *J. Phys. Chem.*, **80**, 829 (1976).

(7) R. B. Hermann, *ibid.*, **76**, 2754 (1972).

(8) "Handbook of Chemistry and Physics," H. C. West, Ed., CRC Press, Cleveland, Ohio, 1970.

(9) L. Pauling, "The Nature of the Chemical Bond," Cornell University Press, Ithaca, N.Y., 1960, p. 260.

(10) J. Traube, *Ann.*, **265**, 27 (1891).

(11) I. Langmuir, *J. Am. Chem. Soc.*, **39**, 1883 (1917).

(12) D. A. Haydon and F. H. Taylor, *Phil. Trans. R. Soc.*, **A252**, 255 (1960).

(13) H. Kimizuka, L. G. Abood, F. Tahara, and K. Kaibara, *J. Colloid Interface Sci.*, **40**, 27 (1972).

(14) J. L. Llopis and P. Artalejo, *An. Fis. Quim. (Madrid)*, **58**, 367 (1962).

(15) M. Nakagaki and T. Handa, *Bull. Chem. Soc., Jpn.*, **48**, 630 (1975).

(16) A. Pullman, H. Berthod, C. Giessner-Pettre, J. F. Hinton, and D. Harpool, *J. Am. Chem. Soc.*, **100**, 3991 (1978).

(17) E. R. Garrett and F. A. Vilallonga, *J. Pharm. Sci.*, **64**, 1782 (1975).

(18) A. F. H. Ward and L. Tordai, *J. Chem. Phys.*, **14**, 453 (1946).

(19) W. Drost-Hansen, in "Chemistry of the Cell Interface," H. Darrow-Brown, Ed., Academic, New York, N.Y., 1971.

(20) M. S. Metzik, V. D. Perevertaev, V. A. Liopo, G. T. Timostchenko, and A. B. Kiseler, *J. Colloid Interface Sci.*, **43**, 662 (1973).

(21) R. E. Phares, *J. Pharm. Sci.*, **54**, 408 (1965).

(22) D. F. Sears, *J. Colloid Interface Sci.*, **29**, 288 (1969).

(23) F. M. Fowkes, *Ind. Eng. Chem.*, **56**, 40 (1964).

(24) M. Poznansky, S. Tong, P. C. White, J. M. Milgram, and A. K. Solomon, *J. Gen. Phys.*, **67**, 45 (1976).
(25) B. E. Cohen, *J. Membrane Biol.*, **20**, 205 (1975).
(26) H. Davson and J. F. Danielli, "The Permeability of Natural Membranes," Cambridge University Press, Cambridge, England, 1941.
(27) B. S. Zwolinski, H. Eyring, and C. E. Reese, *J. Phys. Colloid Chem.*, **53**, 1426 (1949).
(28) S. Glasstone, K. J. Laidler, and H. Eyring, "The Theory of Rate Processes," McGraw-Hill, New York, N.Y., 1941.
(29) Y. Katz and J. M. Diamond, *J. Membrane Biol.*, **17**, 101 (1974).
(30) A. Leo, C. Hansch, and D. Elinns, *Chem. Rev.*, **71**, 525 (1971).
(31) J. Wang, G. T. Tich, W. R. Galey, and A. K. Solomon, *Biochim. Biophys. Acta*, **255**, 691 (1972).
(32) W. D. Stein, "The Movement of Molecules Across Cell Membranes," Academic, New York, N.Y., 1967, p. 76.
(33) H. Hughes, "Physical Chemistry," Pergamon, London, England, 1961, pp. 46, 952, 956.
(34) T. L. Hill, "Introduction to Statistical Thermodynamics," Addison-Wesley, Reading, Mass., 1960, pp. 89, 127.

ACKNOWLEDGMENTS

The authors thank Professor J. R. Sabin for making the CNDO program of the Quantum Theory Project of the University of Florida available.

Protein Concentration Effects on Binding of ^{14}C-Codeine, ^{14}C-Morphine, and ^{3}H-Methadone to Human Serum Albumin

JOSEPH JUDIS

Received February 26, 1979, from the *College of Pharmacy, University of Toledo, Toledo, OH 43606.* Accepted for publication August 8, 1979.

Abstract □ The binding of ^{14}C-codeine, ^{14}C-morphine, and ^{3}H-methadone to human serum albumin was studied at a constant ligand concentration and varying albumin concentrations. Scatchard plots of the data were linear and had positive slopes. The curves for the three ligands had similar data values and slopes. With increasing albumin concentrations, β (fraction bound) values increased. The β change per albumin concentration change $[d(\beta)/d(\text{albumin})]$ dropped most markedly at lower albumin concentrations and changed less as the albumin concentrations approached those normally observed in human blood. Values of nK, the number of binding sites or systems on the protein times the association constant, calculated from β and the albumin concentrations decreased with an increase in albumin concentration increase. The curves were similar for codeine and morphine, while the methadone curve indicated less of a decrease in nK with an increasing albumin concentration. For data published previously on the binding of various ligands at different albumin concentrations, plots of β values or calculated nK values *versus* albumin concentration revealed that β generally increased and nK decreased with an increasing albumin concentration. Desipramine, propoxyphene, prednisone, and phenylbutazone were exceptions to these relationships.

Keyphrases □ Codeine—binding to human serum albumin, varying albumin concentration □ Morphine—binding to human serum albumin, varying albumin concentration □ Methadone—binding to human serum albumin, varying albumin concentration □ Binding, protein—codeine, morphine, and methadone to human serum albumin, varying albumin concentration

In most studies of drug binding to serum proteins, a single protein concentration was used and the ligand concentration was varied (1–3). Scatchard plots of the data gave either a straight line or curve and almost invariably had a negative slope. However, studies of cortisol binding to serum albumin were conducted in which the cortisol concentration was constant and the albumin concentration was varied (4). The resulting Scatchard plot was a straight line with a positive slope. The results could not be explained on the basis of microheterogeneity or by variations of the albumin activity coefficient. This observation was not investigated further.

Several subsequent studies involved the binding of various ligands to serum proteins using a constant ligand concentration and varying protein concentrations. Scatchard plots with a positive slope were observed with thiopental (5), phenytoin (6, 7), and L-tryptophan (6, 7). Bowmer and Lindup (8) recently commented on the several published studies involving data yielding Scatchard plots with positive slopes and the significance of obtaining binding data when the protein concentration is varied and the ligand concentration is constant.

Previous studies involving the binding of ^{14}C-codeine, ^{14}C-morphine, and ^{3}H-methadone to human serum albumin yielded Scatchard plots with positive slopes when the albumin concentration was constant and the ligand concentration was varied (9). No explanation for the positive slopes (rather than the usually observed negative slopes) could be offered. This report is an extension of the earlier studies and involves variation of the albumin concentration and constant ligand concentrations.

EXPERIMENTAL

Methods—All protein binding determinations were performed by the equilibrium dialysis method (9) using multiple-cell blocks. Each cell had 1 ml on each side of the cellulose membrane. Radioactivity was determined in a liquid scintillation system as described previously (9).

Materials—^{14}C-Codeine[1], ^{14}C-morphine[1], ^{3}H-methadone[2], and crystalline human serum albumin[3] were obtained commercially. All chemicals were reagent grade.

RESULTS AND DISCUSSION

The human serum albumin concentration was varied between 0.217×10^{-4} and 0.87×10^{-3} *M*. The ligand concentration was kept constant (^{14}C-morphine, 0.00356; ^{14}C-codeine, 0.00339; and ^{3}H-methadone, 0.00332 *M*). Scatchard plots of the data for the three ligands are shown in Fig. 1. The albumin concentrations for each ligand fell in the same sequence on the curve as found in studies (4, 5, 7) involving a constant ligand concentration and varying albumin concentrations. The slopes

[1] Amersham Corp.
[2] New England Nuclear Corp.
[3] ICN Life Sciences Group.

0022-3549/80/0100-0071$01.00/0